

It follows from (1) that

$$\sum_{l=-\infty}^{+\infty} \left| \sum_{i=1}^N \left\{ J_l(\boldsymbol{\tau} \cdot \mathbf{a}_i) f'_i(\omega + l\Omega) \left[J_l(\boldsymbol{\tau} \cdot \mathbf{a}_i) f'_i(\omega + l\Omega) + 2 \sum_{j=i+1}^N J_l(\boldsymbol{\tau} \cdot \mathbf{a}_j) \{ f'_j(\omega + l\Omega) \cos [\boldsymbol{\tau} \cdot (\mathbf{r}_i - \mathbf{r}_j)] - f''_j(\omega + l\Omega) \sin [\boldsymbol{\tau} \cdot (\mathbf{r}_i - \mathbf{r}_j)] \} \right] \right\} \right|^{1/2} = C_n \quad (3)$$

where

$$C_n = \Delta R^s \omega^2 / \omega_i^2 \exp [-W(\boldsymbol{\tau})].$$

Equation (3) is a system of nonhomogeneous equations with variable coefficients with respect to the functions $\cos(\boldsymbol{\tau} \cdot \mathbf{r}_i)$ and $\sin(\boldsymbol{\tau} \cdot \mathbf{r}_i)$. Therefore, to determine the values of $\cos(\boldsymbol{\tau} \cdot \mathbf{r}_i)$ and $\sin(\boldsymbol{\tau} \cdot \mathbf{r}_i)$ one must have $N(N-1)$ independent equations. In other words, to determine the phases of the X-ray scattering amplitude for the i th atom, the relative increase of the integral reflection coefficients for $N(N-1)$ different values of oscillation amplitudes \mathbf{a}_i must be measured. The values of \mathbf{a}_i can be easily varied by changing the strength of the electric field E of the laser beam or its projection on the scattering plane. The phase of the X-ray reflection φ can be easily derived using the phases of the atomic scattering amplitudes.

It should be noted that a similar method can be used in the case of kinematic diffraction of X-rays. Then the system of equations for the determination of the phases of the X-ray scattering amplitude for the i th atom has the form

$$\sum_{l=-\infty}^{+\infty} \sum_{i=1}^N \left\{ J_l(\boldsymbol{\tau} \cdot \mathbf{a}_i) f'_i(\omega + l\Omega) \left[J_l(\boldsymbol{\tau} \cdot \mathbf{a}_i) f'_i(\omega + l\Omega) + 2 \sum_{j=i+1}^N J_l(\boldsymbol{\tau} \cdot \mathbf{a}_j) \{ f'_j(\omega + l\Omega) \cos [\boldsymbol{\tau} \cdot (\mathbf{r}_i - \mathbf{r}_j)] - f''_j(\omega + l\Omega) \sin [\boldsymbol{\tau} \cdot (\mathbf{r}_i - \mathbf{r}_j)] \} \right] \right\} = B_n \quad (4)$$

where

$$B_n = \Delta R^s \omega^4 / \omega_i^4 \exp [-2W(\boldsymbol{\tau})].$$

Acta Cryst. (1992). **A48**, 281–293

A Crystal-Chemical Model of Atomic Interactions. 6. Intermetallic Phase Structures

BY L. A. ASLANOV AND V. T. MARKOV

Department of Chemistry, Moscow State University, 119899 Moscow, USSR

(Received 28 June 1991; accepted 15 November 1991)

Abstract

Commonly occurring structures are considered from the point of view of a crystal-chemical model of

Clearly (4) permits one to determine the values $\boldsymbol{\tau} \cdot (\mathbf{r}_i + \mathbf{r}_j)$. For their determination one needs to have $N(N-1)$ measurements of the relative integral reflection coefficient of the crystal. Equations (3) and (4) allow one to determine the forced oscillation amplitudes \mathbf{a}_i of the atoms in the crystal with known structure which is very important for several problems of nonlinear optics (Shen, 1984). In this situation, the reciprocal-lattice vector $\boldsymbol{\tau}$ is also a variable parameter.

3. Concluding remarks

The optimization of the experimental conditions in the experiment of Chapman, Hsiesh & Collela (1984) (laser irradiation focusing and changing of crystal orientation) allows one to increase the projection of the electric field strength \mathbf{E} on the reciprocal-lattice vector $\boldsymbol{\tau}$ by at least one order of magnitude. Thus the method proposed seems to be easily realized experimentally.

The authors wish to thank Professor Baryshevsky for numerous discussions and valuable help.

References

- BARYSHEVSKY, V. G. (1982). *Channeling, Radiation and Reactions in Crystals Under High Energies*. Minsk: Izd. Byelorussian Univ.
- BORN, M. & HUANG, K. (1954). *Dynamical Theory of Crystal Lattices*. Oxford: Clarendon Press.
- BUDO, G., DINTRIS, H. M., KENDREW, J. C. & WYCKHOFF, H. W. (1959). *Proc. R. Soc. London Ser. A*, **253**, 70–83.
- CHANG, S.-L. (1984). *Multiple Diffraction of X-rays in Crystals*. Berlin, Heidelberg, New York, Tokyo: Springer-Verlag.
- CHAPMAN, L. D., HSIESH, S. H. & COLLELA, R. (1984). *Phys. Rev. B*, **30**, 1094–1096.
- COLLELA, R. (1982). *Z Naturforsch. Teil A*, **37**, 437–447.
- MÖSSBAUER, R. L., PARAK, F. & HOPPE, W. (1981). In *Mössbauer Spectroscopy 2: the Exotic Side of the Method*, edited by U. GONSER. Berlin, Heidelberg, New York: Springer-Verlag.
- POLIKARPOV, I. V. & SKADOROV, V. V. (1987). *Phys. Status Solidi B*, **143**, 11–17.
- POLIKARPOV, I. V. & SKADOROV, V. V. (1988). *Phys. Status Solidi B*, **149**, 435–439.
- SHEN, Y. R. (1984). *The Principles of Nonlinear Optics*. New York, Chichester Brisbane, Toronto, Singapore: John Wiley.

atomic interactions. It is shown that these structures sometimes contain coordination polyhedra distinct from Platonic, Archimedean and Zalgaller's polyhedra. These polyhedra have two or more groups of

atoms into which all the vertices of the coordination polyhedron can be divided and which differ in distance from the central atom. The reasons for such polyhedra are considered. The crystal structure of NiTi₂ is analyzed and the causes of the quasicrystal state are revealed.

Introduction

The possibilities of the crystal-chemical model of atomic interactions (CCMAI) have been demonstrated for many examples (Aslanov, 1988*a, b*, 1989*a, b*, 1991; Aslanov & Markov, 1989). It was shown that one can apply the CCMAI with equal success to crystals with ionic, covalent and van-der-Waals-type chemical bonds. To do so, we took examples from various classes of chemical compounds. However, it is important to know how fully the CCMAI covers the compounds of each class. This problem is very difficult in general due to the extremely large number of structure types of inorganic compounds. So one of the classes, intermetallic phases, was chosen and a nearly complete check was carried out: all the structure types listed in the handbook of Villars & Calvert (1985) with 50 or more representatives were considered and their crystal-chemical analyses were performed. The intermetallic phases were chosen because their structures are well systematized in this handbook, they have high symmetry as a rule, which speeds up the analysis, and they contain unusual polyhedra which do not belong to the groups of Platonic regular solids (PRS), Archimedean semiregular solids (ASRS) and Zalgaller's polyhedra (ZP) and so need to be understood in the framework of CCMAI.

A series of structure types has already been considered (Aslanov, 1988*a, b*, 1991; Aslanov & Markov, 1989), *e.g.* MgCu₂, Cr₃Si *etc.* We present below the crystal-chemical analysis of the rest of the structure types of intermetallic phases, except for BFe and BCr which have 106 and 165 representatives respectively. Their structures have chains of atoms $\cdots\text{B-B}\cdots$, which determine the peculiarities of these two structure types.

In the text below, the formula of every structure type is followed by a number in parentheses. This is the number of compounds which have the same structure type according to the handbook by Villars & Calvert (1985). The symbols or names of atoms belonging to a coordination sphere are accompanied in parentheses by the distances of these atoms from the center of the complex and the number of these atoms after the multiplication sign.

In line with the notation of an earlier paper (Aslanov & Markov, 1989) Zalgaller's polyhedra (ZP) are denoted by the number assigned in the book by Zalgaller (1969), for example (ZP no. 14).

Structures with unusual polyhedra in the first coordination sphere

We have found only three unusual polyhedra and five structure types having such polyhedra of the 27 structures considered below. It shows that polyhedra distinct from PRS, ASRS and ZP are very rare.

The causes of the formation of unusual coordination polyhedra can be explained taking b.c.c. structures as an example. It was shown previously (Aslanov, 1988*a*) that the energies of interaction of the central atom with the atoms in the first and second coordination spheres are approximately equal and are little different from the interaction energy in the hypothetical case when the distance from the central atom to the atoms of the first coordination sphere is equal to the distance corresponding to the minimum of the curve of diatomic interaction energy. The combination of two coordination spheres gives a rhombidodecahedron, which one may consider (as is done in many cases in the literature) as a polyhedron of the first coordination sphere with the special feature that its vertices are inscribed in two spheres of different radii. One can suppose in principle that there also exist other coordination polyhedra whose vertices may be divided into two or more groups such that each group is characterized by its own distance from the center. We shall call such polyhedra multi-spheric. The condition of formation of such polyhedra is the shallowness of the atomic interaction curve in the neighborhood of its minimum. In other words, the minimum of such a curve has to be sufficiently wide. This means that one searches for such polyhedra first in compounds in which at least one atom is a metal with b.c.c. or in the last resort h.c.p. structure.

The second factor which assists the formation of unusual polyhedra is a large difference between the radii of the central atom and the atoms in the first coordination sphere. As a rule, the central atom in the unusual polyhedra is big and the atoms in the first coordination sphere are relatively small. In the compounds considered below the metallic radii (in Å) of the atoms in question and their ratios (for the sake of compatibility the radii for coordination number 12 are used) are (Wells, 1984): Ba:Al = 2.24:1.43 = 1.57; Ca:Cu = 1.97:1.28 = 1.54; Th:Mn = 1.80:1.37 = 1.31 (or Th:Ni = 1.80:1.25 = 1.44); Nb:Be = 1.47:1.12 = 1.31.

Al₄Ba (454). The structural ensemble consists of two complexes. One of these has the Ba atom in the center of the only coordination sphere which is a polyhedron (Fig. 1*a*) with 18 Al atoms at the vertices: Al(2) (3.48 Å × 8, for vertices *D* and *E* in Fig. 1*a*); Al(1) (3.60 Å × 8, for vertices *B* and *C*); Al(2) (4.24 Å × 2, for vertex *A*). The lengths of all edges of this polyhedron are practically equal: *AB* = 2.69; *BD* = 2.69, *DE* = 2.68 Å. The short diagonals *BC* of the rhombus-shaped faces are substantially longer

(3.21 Å). This polyhedron should be considered as two semirhombidodecahedra moved apart a distance equal to the length of the rhombidodecahedron edge. The interatomic distances Al-Al of 2.68–2.69 Å in Al_4Ba are a little less than that in pure aluminium, 2.86 Å.

The second complex of the structural ensemble has atom Al(1) in the center and two coordination spheres. Atoms Al(2) ($2.69 \text{ \AA} \times 4$) form a tetrahedron (Fig. 1b) in the first coordination sphere. Atoms Ba (3.60×4) and Al(1) ($3.21 \text{ \AA} \times 4$) are distributed at the vertices of the gyrobifastigium (Fig. 1c, ZP no. 26). Atoms Al(1) are at the corners of the equatorial square and the Ba atoms are above and below this square. The atoms of the second coordination sphere and atoms Al(1) of the first complex are the centers of the new structural ensembles.

ThMn_{12} (132). The structural ensemble consists of one complex with the Th atom in the center and three coordination spheres. The first one contains 20 Mn atoms (Fig. 2a): Mn(3) ($3.15 \text{ \AA} \times 8$); Mn(2) ($3.16 \text{ \AA} \times 4$); Mn(1) ($3.33 \text{ \AA} \times 8$). The polyhedron looks like two semicuboctahedra moved apart with a square with atoms Mn(2) at the corners inserted between.

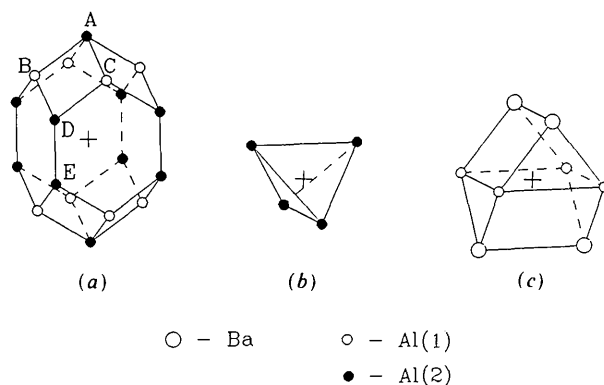


Fig. 1. Structural ensemble Al_4Ba . Complex I with the Ba atom at the center: (a) the only coordination sphere. Complex II with atom Al(1) at the center: (b) and (c) the first and second coordination spheres.

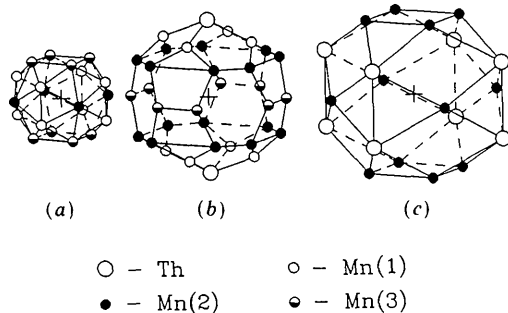


Fig. 2. Structural ensemble ThMn_{12} . The Th atom is at the center: (a), (b) and (c) the first, second and third coordination spheres.

The polyhedron of the Ba atom in Al_4Ba (Fig. 1a) can be transformed into the thorium polyhedron (Fig. 2a) in ThMn_{12} if atoms are added above the centers of the hexagonal faces and the vertices A are ignored (Fig. 1a).

The edges of the polyhedron slightly differ in length: Mn(1)–Mn(1) $2.48 \text{ \AA} \times 4$; Mn(1)–Mn(3) $2.52 \text{ \AA} \times 16$; Mn(1)–Mn(2) $2.69 \text{ \AA} \times 16$; Mn(2)–Mn(3) $2.71 \text{ \AA} \times 8$; Mn(3)–Mn(3) $2.76 \text{ \AA} \times 8$. The difference in the distances Mn–Mn ($\sim 10\%$) is smaller than in the α -Mn structure (2.26–2.93 Å) (Wells, 1984), which is stable at the same temperature.

The polyhedron of the second coordination sphere (Fig. 2b) is a dual one to the polyhedron of the first coordination sphere. It contains 34 atoms: Mn(1) ($4.83 \text{ \AA} \times 8$); Th ($4.95 \text{ \AA} \times 2$); Mn(3) ($5.00 \text{ \AA} \times 8$); Mn(2) ($5.17 \text{ \AA} \times 16$). This polyhedron has four hexagonal and eight pentagonal faces; additionally it has eight pentagonal faces bent along the diagonal at an angle of approximately 15° (Fig. 2b).

The polyhedron of the third coordination sphere (Fig. 2c) is dual to the previous one and is nearly identical to the polyhedron of the first coordination sphere. The atoms at its vertices are: Mn(2) ($5.58 \text{ \AA} \times 4$); Mn(2) ($5.87 \text{ \AA} \times 8$); Th ($6.66 \text{ \AA} \times 8$). Eight Th atoms of the third coordination sphere and two Th atoms of the second sphere are the centers of the new trispheric complexes.

CaCu_5 (277). The structural ensemble consists of a single complex with a Ca atom at the center and two coordination spheres. The first coordination sphere is an unusual polyhedron, viz a hexagonal prism with caps above quadrilateral faces (Fig. 3a). 18 Cu atoms are at the vertices of this polyhedron: Cu(2) ($3.26 \text{ \AA} \times 12$); Cu(1) ($2.94 \text{ \AA} \times 6$). The lengths of the edges are $2.55 \text{ \AA} \times 12$ (hexagonal faces) and $2.52 \text{ \AA} \times 24$ (all others). These data coincide with the interatomic distance 2.55 \AA in pure copper. So maximal coordination number of the Ca atom and a minimum of the potential energy of the complex CaCu_{18} are possible, provided the coordination polyhedron consists of two groups of atoms with different distances Ca–Cu.

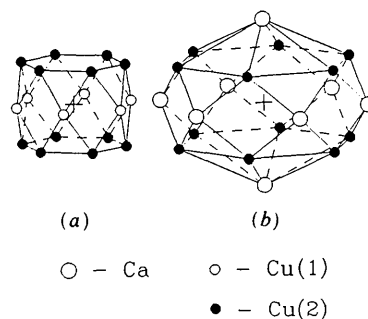


Fig. 3. Structural ensemble CaCu_5 . The Ca atom is at the center: (a) and (b) the first and second coordination spheres.

The second coordination sphere of the structural ensemble (Fig. 3b) is a polyhedron with 20 vertices which is dual to the polyhedron of the first coordination sphere. It contains two fragments – a hexagonal prism with atoms Cu(2) ($4.86 \text{ \AA} \times 12$) at the vertices and a hexagonal bipyramid of Ca atoms ($5.09 \text{ \AA} \times 6$, $4.09 \text{ \AA} \times 2$). From a geometrical point of view, the cap over the hexagonal face is impossible, but it should be noted that the hexagon is built of Cu atoms and a larger Ca atom is at the top of the cap and the center of the structural ensemble is filled with another Ca atom.

Th₂Ni₁₇ (87). The structural ensemble consists of two trispheric complexes with atoms Th(1) and Th(2) at their centers. The second Th atom has a more regular polyhedron in the third sphere so it is worth beginning with this complex. Atom Th(2) is surrounded (Fig. 4a) with atoms Ni(2) ($3.16 \text{ \AA} \times 6$) and Ni(4) ($3.16 \text{ \AA} \times 6$) which form a hexagonal prism. The atoms Ni(3) ($2.79 \text{ \AA} \times 6$) are over the quadrilateral faces of the hexagonal prism at the tops of the caps. The polyhedron with 18 vertices has two types of edges: around hexagonal faces, $2.47 \text{ \AA} \times 12$, and between hexagonal faces and the tops of the caps, $2.42 \text{ \AA} \times 24$. The interatomic distance in pure nickel is 2.49 \AA .

The second coordination sphere (Fig. 4b) is dual relative to the previous one if one takes into account the fact that the rhombus-shaped faces of the polyhedron in the first coordination sphere are covered in the next but one by pairs of atoms Ni(1) (4.96×6) in a such way that each atom of these two is situated over the triangular semirhombus. The centers of three

other rhombus-shaped faces are covered with atoms Th(1) ($4.83 \text{ \AA} \times 3$). All these atoms belong to the polyhedron (Fig. 4b) with 23 atoms: Ni(1) (2.93×2) at the apical positions, Ni(4) ($4.65 \text{ \AA} \times 12$) at the vertices of the hexagonal prism and all others as described above.

The third coordination sphere (Fig. 4c) contains atoms Ni(3) ($5.58 \text{ \AA} \times 6$), Th(1) ($6.32 \text{ \AA} \times 6$) and Th(2) ($6.32 \text{ \AA} \times 6$) at the vertices of the polyhedron which is dual to the previous one. The Th atoms form a hexagonal prism and the Ni atoms are distributed at the tops of the caps over the quadrilateral faces of the hexagonal prism.

The complex with atom Th(1) at its center has a polyhedron with 18 vertices as a first coordination sphere (Fig. 4d). This is the same polyhedron as the polyhedron of the Th(2) atom. Atoms Ni(4) ($3.16 \text{ \AA} \times 12$) form the hexagonal prism and atoms Ni(3) ($2.79 \text{ \AA} \times 6$) are over the quadrilateral faces. The lengths of edges are $2.42 \text{ \AA} \times 12$ around hexagonal faces and $2.78 \text{ \AA} \times 24$ between the vertices of the hexagonal prism and the caps.

The coordination polyhedron of the second coordination sphere repeats (Fig. 4e) the respective polyhedron of the previous complex with atom Th(2) at its center, but apical atoms Th(1) ($4.07 \text{ \AA} \times 2$) are pushed out of the center because of the larger radius of the Th atom in comparison to Ni(1) atoms in a complex with Th(2) at the center. Atoms Ni(2) ($4.65 \text{ \AA} \times 12$) form the hexagonal prism, atoms Th(2) ($4.83 \text{ \AA} \times 3$) are at the vertices of the single caps and atoms Ni(1) ($4.96 \text{ \AA} \times 6$) are at the vertices of the double caps over the rhombus-shaped faces of the polyhedron in the first coordination sphere. The polyhedron of the third coordination sphere is distorted (Fig. 4f), but in fact is dual to the previous polyhedron. The distortion is a consequence of the shift of the atoms Th(1) from the center in the polyhedron of the second coordination sphere and the different atoms at the vertices of the hexagonal prism. The hexagonal faces with atoms Ni(1) ($5.65 \text{ \AA} \times 6$) and Th(2) ($6.32 \text{ \AA} \times 6$) at the corners are bent along short diagonals because Ni(1) and Th(2) alternate in both hexagons. Atoms Ni(3) ($5.58 \text{ \AA} \times 6$) are at the tops of the caps over the quadrilateral faces.

Be₃Nb (70). The structural ensemble consists of two complexes with atoms Nb(1) and Nb(2) in the centers. Atom Nb(1) is surrounded by atoms Be(3) ($2.86 \text{ \AA} \times 12$) at the vertices of a hexagonal prism; atoms Be(2) ($2.63 \text{ \AA} \times 6$) are over the quadrilateral faces (Fig. 5a). This polyhedron is the same as in the previous two structures. The edge lengths around the hexagonal faces are 2.33 and 2.22 \AA (the long edges alternate with the short ones) and edges connecting the vertices of the hexagonal prism with caps have length 2.16 \AA (on average). The interatomic distance in metallic beryllium is 2.22 \AA .

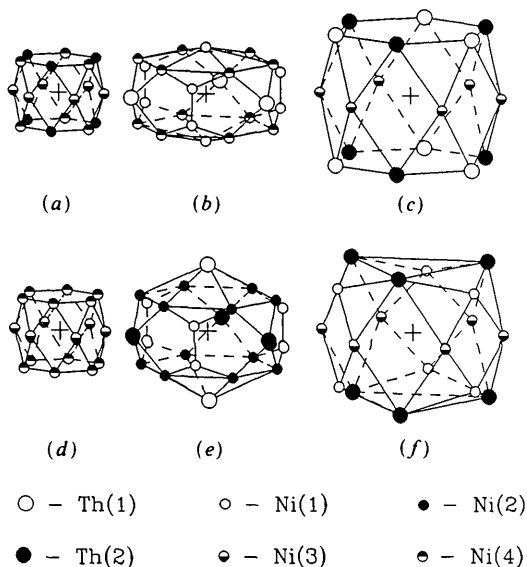


Fig. 4. Structural ensemble Th₂Ni₁₇. Complex I with atom Th(2) at the center: (a), (b) and (c) the first, second and third coordination spheres. Complex II with atom Th(1) at the center: (d), (e) and (f) the first, second and third coordination spheres.

The second and third coordination spheres (Figs. 5*b, c*) are the same as in the structural ensemble $\text{Th}_2\text{Ni}_{17}$. The second coordination sphere (Fig. 5*b*) consists of atoms Nb(2) ($2.95 \text{ \AA} \times 2$) at the apical positions, Nb(1) ($4.56 \text{ \AA} \times 6$) at the equatorial positions, Be(3) ($4.28 \text{ \AA} \times 6$, $4.34 \text{ \AA} \times 6$) at the vertices of the hexagonal prism and the third (Fig. 5*c*) consist of atoms Nb(2) ($5.43 \text{ \AA} \times 12$) at the vertices of the hexagonal prism and Be(2) ($5.27 \text{ \AA} \times 6$) at the tops of the caps.

The first coordination sphere (Fig. 5*d*) of Nb(2) has the atoms Be(3) ($2.59 \text{ \AA} \times 6$, $2.67 \text{ \AA} \times 3$) and Be(1) ($2.69 \text{ \AA} \times 3$) at the vertices of the truncated tetrahedron. Atoms Nb(1) (2.95 \AA) and Nb(2) ($2.86 \text{ \AA} \times 3$) form the tetrahedron in the second coordination sphere (Fig. 5*e*).

$\text{Th}_2\text{Zn}_{17}$ (65). The structural ensemble has minimal differences from the structural ensemble $\text{Th}_2\text{Ni}_{17}$. It consists of one trispheric complex with a Th atom in the center. The first coordination sphere (Fig. 6*a*) is a polyhedron with 18 vertices like the polyhedrons in the structures CaCu_5 , $\text{Th}_2\text{Ni}_{17}$ and Be_3Nb . It has atoms Zn(4) ($3.41 \text{ \AA} \times 9$) and Zn(2) ($3.41 \text{ \AA} \times 3$) at the vertices of the hexagonal prism and atoms Zn(3) ($3.01 \text{ \AA} \times 6$) at the tops of the caps over the quadrilateral faces of the hexagonal prism. The edge lengths are 2.61 \AA (hexagonal faces) and 2.67 \AA (caps). They are close to the smallest interatomic distance in metallic zinc (2.66 \AA).

The polyhedron of the second coordination sphere (Fig. 6*b*) has different atoms at the apical positions, *viz* Th (4.40 \AA) and Zn(1) (3.12 \AA). This explains the

distortions of the polyhedron in the next coordination sphere. The polyhedron of the second coordination sphere has a hexagonal prismatic fragment with atoms Zn(2) ($5.02 \text{ \AA} \times 6$) and Zn(4) ($5.02 \text{ \AA} \times 6$) at the vertices. The single caps over the quadrilateral faces are atoms Th ($5.21 \text{ \AA} \times 3$), the double caps are atoms Zn(1) ($5.37 \text{ \AA} \times 6$).

Before the third coordination sphere is considered, it is worth noting that the polyhedron of the third coordination sphere in the structural ensemble $\text{Th}_2\text{Ni}_{17}$ is distorted in the complex with Th(1) at the center. This complex has the Th atoms at the apical positions of the second-ordination-sphere polyhedron.

The distortion of the third-ordination-sphere polyhedron $\text{Th}_2\text{Zn}_{17}$ exists only on the side which has contact with the Th atom in the apical position of the second-ordination-sphere polyhedron (Fig. 6*c*). The hexagonal prism has a regular hexagonal face with Th atoms ($6.82 \text{ \AA} \times 6$) at the vertices. The distorted hexagonal face has both Th atoms ($6.82 \text{ \AA} \times 3$) and Zn(1) atoms ($6.08 \text{ \AA} \times 3$). Atoms Zn(3) ($6.02 \text{ \AA} \times 6$) are at the cap tops.

This is the end of the description of the structural ensemble $\text{Th}_2\text{Zn}_{17}$ but another aspect of this structure should be considered to explain the similarity of the crystal structures $\text{Th}_2\text{Zn}_{17}$, CrFe and Mn_5Si_3 discussed below.

There is a diatomic cluster (Fig. 6*d*) which has an interatomic distance for Zn(1) of 2.56 \AA , which is shorter than that in metallic zinc (2.66 \AA). The coordination polyhedron of this cluster is the same as the polyhedron of the Th atom described above (Fig. 6*e*).

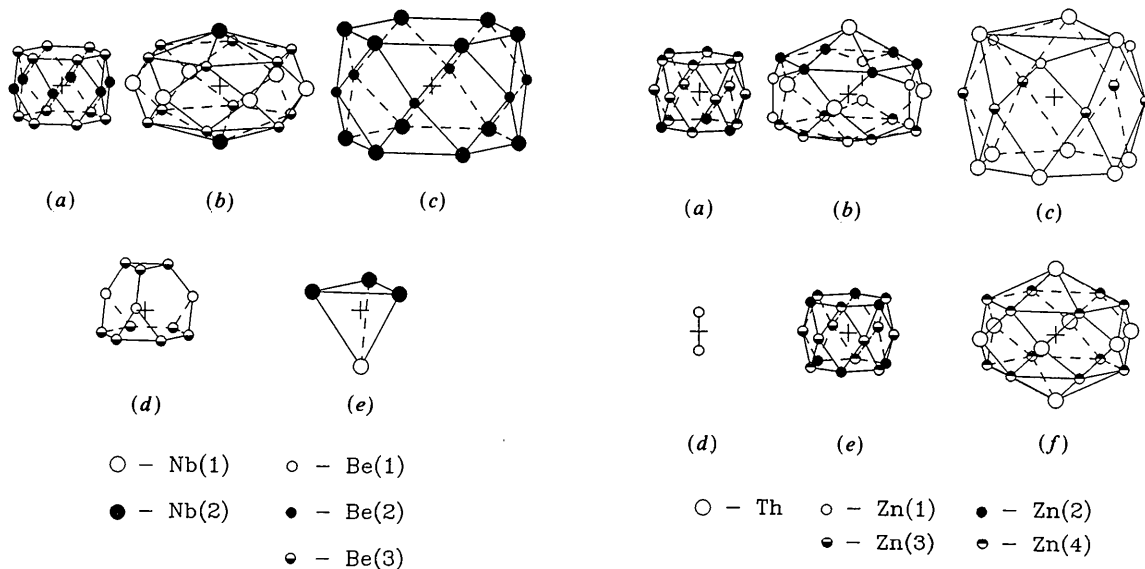


Fig. 5. Structural ensemble Be_3Nb . Complex I with atom Nb(1) at the center: (a), (b) and (c) the first, second and third coordination spheres. Complex II with atom Nb(2) at the center: (d) and (e) the first and second coordination spheres.

Fig. 6. Structural ensemble $\text{Th}_2\text{Zn}_{17}$. The Th atom is at the center: (a), (b) and (c) the first, second and third coordination spheres. The second aspect: (d) the diatomic cluster in the center; (e) and (f) the first and second coordination spheres of the diatomic cluster.

The hexagonal prism has atoms Zn(4) ($3.41 \text{ \AA} \times 6$) and Zn(2) ($3.41 \text{ \AA} \times 6$) at the vertices and atoms Zn(3) ($3.01 \text{ \AA} \times 6$) at the tops of the caps. The second coordination sphere (Fig. 6f) is a polyhedron with 20 vertices that was described in the structure CaCu₅ (3b). The Th atoms are at the apical and equatorial positions ($4.40 \text{ \AA} \times 2$ and $5.21 \text{ \AA} \times 6$ respectively). Atoms Zn(4) ($5.02 \text{ \AA} \times 12$) form the hexagonal prism.

Structures with the ordinary polyhedra

(a) Structures with diatomic clusters at the center of the complex

CrFe (84). This structural type is another example of a diatomic cluster inside a polyhedron with 18 vertices which is considered in this structure as a combination of two hexagonal antiprisms with atoms $M(3)$ at the centers, hence it is discussed in this section.

The sixfold pseudoaxis of the polyhedron with 18 vertices coincides with the infinite-fold axis of the diatomic cluster (Fig. 7). The Cr and Fe atoms are indistinguishable (Villars & Calvert, 1985), so all atoms are denoted M ; there is no possibility of comparing the interatomic distances in this structure to those in pure chromium or iron.

The structural ensemble consists of two complexes. One has the diatomic cluster (Fig. 7a) in the center with interatomic distance $M(3)-M(3) = 2.40 \text{ \AA}$, i.e.

the shortest interatomic distances in different polymorphs of chromium or iron are larger: 2.50 \AA α -Cr; 2.72 \AA β -Cr; 2.48 \AA α -Fe; 2.51 \AA β -Fe; 2.54 \AA σ -Fe. The coordination polyhedron of the cluster (Fig. 7b) has atoms $M(4)$ ($3.23 \text{ \AA} \times 4$) and $M(5)$ ($3.42 \text{ \AA} \times 8$) at the vertices of the hexagonal prism and atoms $M(4)$ ($2.29 \text{ \AA} \times 2$) and $M(3)$ ($2.57 \text{ \AA} \times 4$) at the tops of the caps over the quadrilateral faces of the hexagonal prism. Only two rhombus-shaped faces of this polyhedron with 18 vertices are flat. Four others are bent along larger diagonals. These distortions are combined with the short distances between atoms $M(4)$ indicated by arrows in Fig. 7(b) and the center of the cluster.

The polyhedron of the second coordination sphere (Fig. 7c) is dual to the previous one. In a contrast to the structural ensembles of CaCu₅, Th₂Ni₁₇, Be₃Nb and Th₂Zn₁₇, this polyhedron is distorted strongly, which is expected considering the distortions of the polyhedron in the first coordination sphere. Atoms $M(2)$ ($3.61 \text{ \AA} \times 2$) are in the apical positions; the hexagonal prism is formed by atoms $M(1)$ (4.40×2), $M(4)$ ($4.40 \text{ \AA} \times 2$) and $M(5)$ ($4.69 \text{ \AA} \times 8$). There are four single caps $M(2)$ ($4.27 \text{ \AA} \times 4$) over the bent rhombus-shaped faces of the first-ordination-sphere polyhedron and two double caps $M(3)$ ($4.70 \text{ \AA} \times 4$) over the flat rhombus-shaped faces of the same polyhedron.

The second complex has atom $M(1)$ at the center and atoms $M(4)$ ($2.25 \text{ \AA} \times 4$), $M(5)$ ($2.54 \text{ \AA} \times 4$) and $M(2)$ ($2.60 \text{ \AA} \times 4$) at the vertices of the distorted icosahedron in the first coordination sphere (Fig. 7d). The atoms $M(3)$ ($3.97 \text{ \AA} \times 8$, $4.24 \text{ \AA} \times 4$) and $M(5)$ ($4.10 \text{ \AA} \times 8$) form the distorted dodecahedron in the second coordination sphere (Fig. 7e). The centers of the diatomic clusters and atoms $M(1)$ form an octahedron; the vertices of this octahedron are the centers of the new complexes. The description of this structure is difficult because of the distortions.

$M_5\text{Si}_3$ (264). The structural ensemble is a bispheric complex with the diatomic cluster Mn₂ in the center (Fig. 8a). Atoms Mn(1) are distributed along the c axis with interatomic spacing 2.41 \AA . Consideration of the diatomic clusters Mn(1)-Mn(1) is useful for a general approach to this structure.

The first coordination sphere of the diatomic cluster is the distorted polyhedron with 18 vertices (Fig. 8b). The atoms Si ($3.20 \text{ \AA} \times 6$) and Mn(2) ($3.62 \text{ \AA} \times 6$) form a distorted hexagonal prism. In fact all quadrilateral faces have caps, but three of them are in the planes of these faces (Si atoms, $2.11 \text{ \AA} \times 3$). Three other quadrilateral faces have real caps with atoms $M(2)$ ($2.70 \text{ \AA} \times 3$) at the top. These three atoms are aside the normals to the quadrilateral faces passing through the center of the complex, so one of the faces of the cap coincides with the adjacent quadrilateral face.

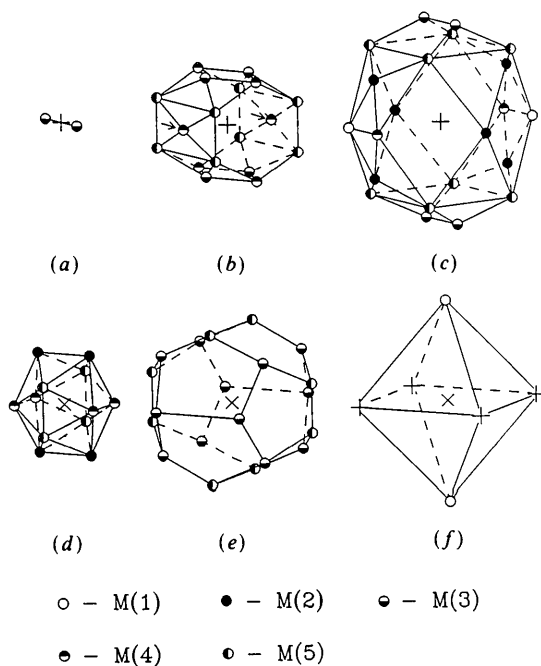


Fig. 7. Structural ensemble CrFe. Complex I: (a) the cluster M_2 is at the center; (b) and (c) the first and second coordination spheres; the atoms nearest to the center are marked with arrows. Complex II with atom $M(1)$ at the center; (d) and (e) the first and second coordination spheres; (f) the distribution of the cluster center and atoms $M(1)$ around the complex II.

The second coordination sphere (Fig. 8c) contains 20 atoms: Si ($4.86 \text{ \AA} \times 3$), $M(2)$ ($4.31 \text{ \AA} \times 3$), Mn(1) ($3.61 \text{ \AA} \times 2$), Mn(1) ($4.17 \text{ \AA} \times 6$), Mn(2) ($4.94 \text{ \AA} \times 6$). The polyhedron is greatly distorted in comparison with the corresponding polyhedron of the structure CaCu_5 (Fig. 3b). The centers of the diatomic clusters are distributed around the complex at the vertices of ZP no. 14 (Fig. 8d).

(b) *Compounds with composition AB_2*

MgZn_2 (400). The structural ensemble is a bispheric complex with an Mg atom at the center. In the first coordination sphere (Fig. 9a), the Zn atoms are distributed at the vertices of a truncated tetrahedron ($3.05 \text{ \AA} \times 12$) and, in the second, four Mg atoms ($3.18 \text{ \AA} \times 4$) form a tetrahedron (Fig. 9b).

AlB_2 (253). The structural ensemble is a bispheric complex with an Al atom in the center. In the first coordination sphere (Fig. 10a), the B atoms form a

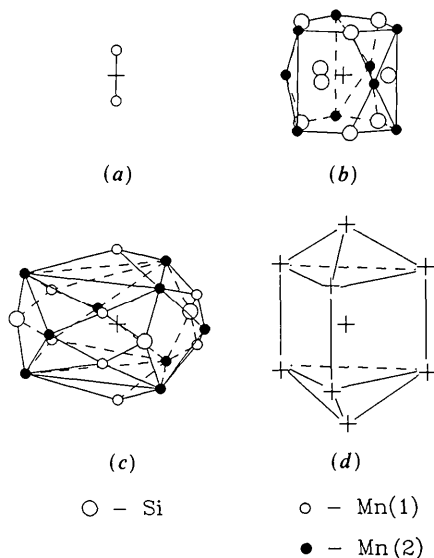


Fig. 8. Structural ensemble Mn_5Si_3 : (a) the cluster Mn_2 is at the center; (b) and (c) the first and second coordination spheres; (d) the distribution of the adjacent diatomic cluster centers.

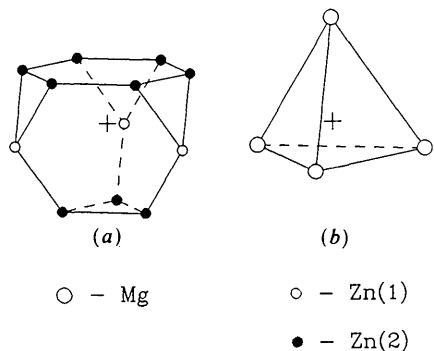


Fig. 9. Structural ensemble MgZn_2 . The Mg atom is at the center: (a) and (b) the first and second coordination spheres.

hexagonal prism ($2.38 \text{ \AA} \times 12$) and in the second (Fig. 10b) the eight Al atoms ($3.01 \text{ \AA} \times 6$, $3.25 \text{ \AA} \times 2$) are distributed on the vertices of a hexagonal bipyramid which is dual to the hexagonal prism of the first coordination sphere.

Co_2Si (363). The structural ensemble consists of some complex with an Si atom in the center and two coordination spheres. In the first (Fig. 11a), the ten Co atoms occupy the vertices of the sphenocorona (ZP no. 86): Co(2) ($2.32 \text{ \AA} \times 3$, 2.35 \AA , 2.62 \AA) and Co(1) ($2.34 \text{ \AA} \times 2$, 2.47 \AA , $2.57 \text{ \AA} \times 2$). In the second coordination sphere (Fig. 11b), the Si atoms ($3.15 \text{ \AA} \times 4$) are placed at the vertices of a distorted tetrahedron.

Fe_2P (264). The structural ensemble consists of some bispheric complex with a P(2) atom at the center. In the first coordination sphere (Fig. 12a),

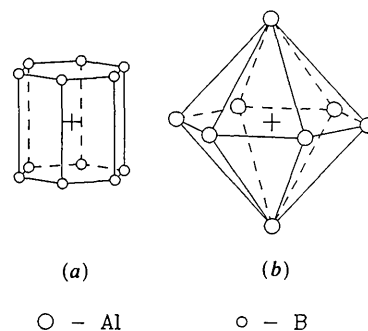


Fig. 10. Structural ensemble AlB_2 . The Al atom is at the center: (a) and (b) the first and second coordination spheres.

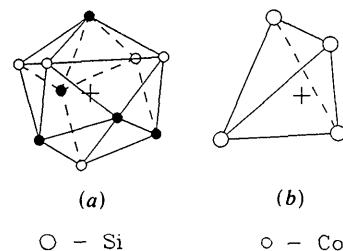


Fig. 11. Structural ensemble Co_2Si . The Si atom is at the center: (a) and (b) the first and second coordination spheres.

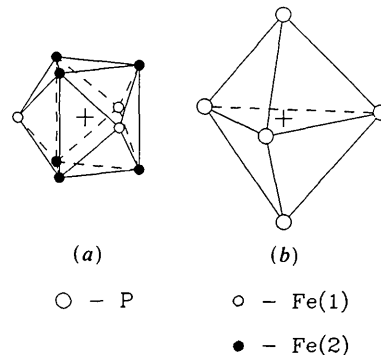


Fig. 12. Structural ensemble Fe_2P . Atom P(2) is at the center: (a) and (b) the first and second coordination spheres.

Fe(2) atoms form a trigonal prism ($2.48 \text{ \AA} \times 6$) and three more atoms Fe(1) ($2.22 \text{ \AA} \times 3$) occupy the vertices of the caps over rectangular faces. In the second coordination sphere (Fig. 12b), the P(2) atoms ($3.39 \text{ \AA} \times 3$, $3.46 \text{ \AA} \times 2$) form a trigonal bipyramid.

Cu_2Sb (194). The structures of this type were considered earlier (Aslanov, 1989b), with Fe_2As as an example.

MoSi_2 (84). The structural ensemble consists of one complex with an Mo atom at the center and five coordination spheres. Basically, the distribution of atoms in this structure is very close to that of a b.c.c. structure but it differs by the distribution of the Mo and Si atoms at the occupied positions. In the first coordination sphere (Fig. 13a), ten Si atoms ($2.61 \text{ \AA} \times 10$) form an elongated tetragonal bipyramid (ZP no. 15). Four MO atoms ($3.20 \text{ \AA} \times 4$) of the second coordination sphere (Fig. 13b) form a square in the equatorial plane which combines with the elongated tetragonal bipyramid to form a distorted rhombidodecahedron. Then there is a cuboctahedron (Fig. 13c) compressed along one of the fourfold axes; it is dual to the rhombidodecahedron and consists of eight Si atoms ($4.13 \text{ \AA} \times 8$) and four Mo atoms ($4.53 \text{ \AA} \times 4$). In the fourth coordination sphere (Fig. 13d), the Si atoms ($5.23 \text{ \AA} \times 8$) form a cube compressed along a fourfold axis and, in the fifth, sixteen Si atoms ($5.23 \text{ \AA} \times 16$) and eight Mo atoms ($4.53 \text{ \AA} \times 8$) are placed at the vertices of a rhombidodecahedron (Fig. 13e) apart from a compression along a fourfold axis.

Al_2Cu (101). The structural ensemble consists of one trispheric complex with a Cu atom in the center. In the first coordination sphere (Fig. 14a), eight Al atoms form a tetragonal antiprism ($2.60 \text{ \AA} \times 8$) and two Cu atoms ($2.44 \text{ \AA} \times 2$) combine to form the

gyroelongated square bipyramid (ZP no. 16). In the second coordination sphere (Fig. 14b), 16 Al atoms ($4.25 \text{ \AA} \times 8$, $4.22 \text{ \AA} \times 8$) form a polyhedron dual to the former. Eight atoms, situated close to the equatorial plane orthogonal to a fourfold axis, are shifted from the central normals to the triangular faces of the antiprism of the first coordination sphere, *i.e.* there are noticeable distortions of the polyhedron caused because these eight atoms belong to the first coordination spheres of the neighbor complexes and the longest edges of the polyhedron, *e.g.* AB , are the body diagonals of the neighbor tetragonal antiprism. In the third coordination sphere (Fig. 14c), the Cu atoms ($4.29 \text{ \AA} \times 4$) form a square.

Although the compositions of B_3Cr_5 and Si_3W_5 are not of type AB_2 , these structure types are similar to that of Al_2Cu .

B_3Cr_5 (54). The structural ensemble consists of two complexes, one of which is trispheric and the other monospheric. In the first complex with a B(1) atom at the center, eight Cr(2) atoms ($2.30 \text{ \AA} \times 8$) form a tetragonal antiprism and two Cr(1) atoms ($2.66 \text{ \AA} \times 2$) combine with it to form the gyroelongated square bipyramid (ZP no. 16) in the first coordination sphere (Fig. 15a). In the second coordination sphere (Fig. 15b), the B(2) atoms ($3.43 \text{ \AA} \times 8$) and the Cr(2) atoms ($3.90 \text{ \AA} \times 8$) are situated at the vertices of a polyhedron dual to that of the first coordination sphere. This 16-vertex polyhedron is distorted exactly as in the Al_2Cu structure. The third coordination sphere of this complex (Fig. 15c) is a square formed by B(1) atoms ($3.86 \text{ \AA} \times 4$).

The second complex with a Cr(1) atom at the center has the single coordination sphere (Fig. 15d) which consists of five B atoms situated at the vertices of a trigonal bipyramid. The B(2) atoms ($2.16 \text{ \AA} \times 3$) are in the equatorial plane and the B(1) atoms ($2.66 \text{ \AA} \times 2$) occupy the apical positions.

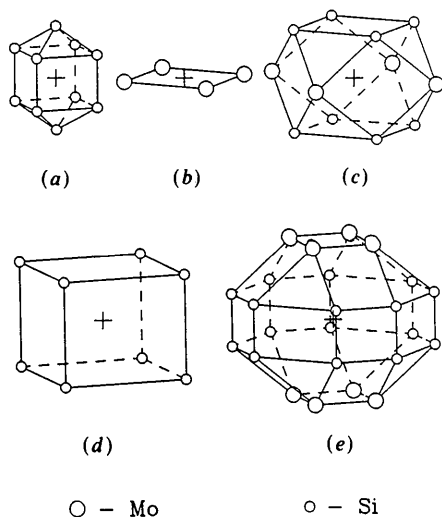


Fig. 13. Structural ensemble MoSi_2 . The Mo atom is at the center: (a)–(e) the first to fifth coordination spheres.

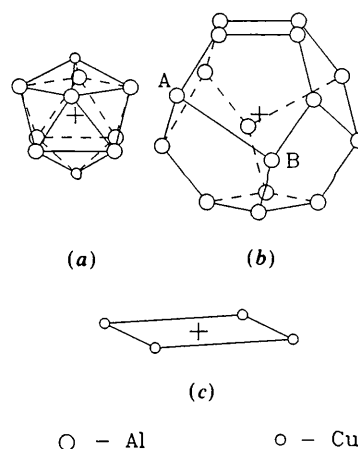


Fig. 14. Structural ensemble Al_2Cu . The Cu atom is at the center: (a), (b) and (c) the first to third coordination spheres.

Si_3W_5 (75). The structural ensemble consists of two complexes. The first one has an Si(1) atom at the center and three coordination spheres. In the first coordination sphere (Fig. 16a), eight W(2) atoms ($2.67 \text{ \AA} \times 8$) form a tetragonal antiprism and two Si(1) atoms ($2.48 \text{ \AA} \times 2$) combine to give the gyroelongated square bipyramid (ZP no. 16). In the second coordination sphere (Fig. 16b), the Si(2) atoms ($3.79 \text{ \AA} \times 8$) and the W(2) atoms ($4.41 \text{ \AA} \times 8$) form a polyhedron dual to the preceding one. The distortions of this

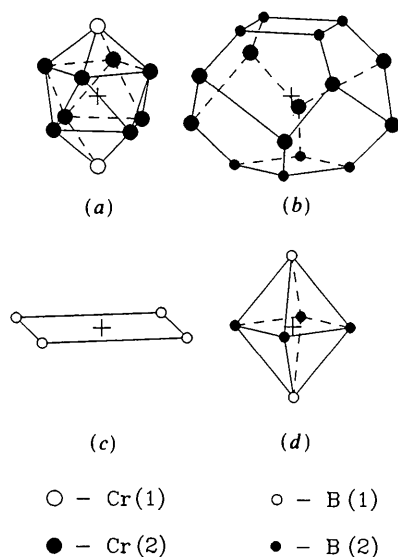


Fig. 15. Structural ensemble B_3Cr_5 . Complex I with atom B(1) at the center: (a), (b) and (c) the first to third coordination spheres. Complex II with atom Cr(1) at the center: (d) the only coordination sphere.

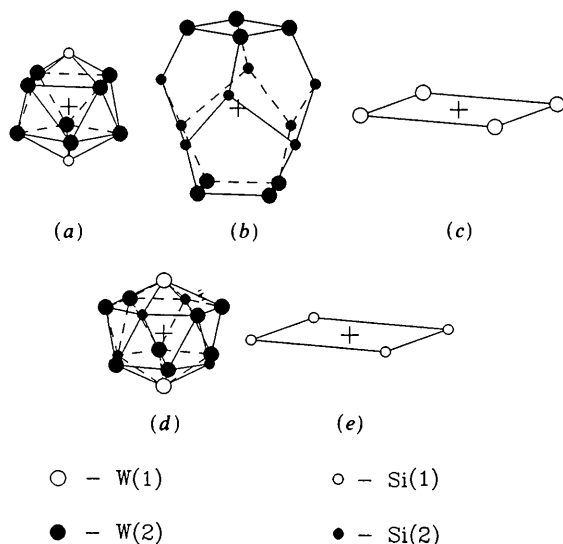


Fig. 16. Structural ensemble Si_3W_5 . Complex I with the atom Si(1) at the center: (a), (b) and (c) the first to third coordination spheres. Complex II with atom W(1) at the center: (d) and (e) the first and second coordination spheres.

polyhedron are negligible in comparison to those of similar polyhedra in Al_2Cu or B_3Cr_5 . The explanation is that the third coordination sphere (Fig. 16c) contains W(1) ($4.82 \text{ \AA} \times 4$) and not Si(1) atoms and the W(1) atom has an environment which is not a tetragonal antiprism.

In the first coordination sphere (Fig. 16d) of the second complex with a W(1) atom at the center, four Si(2) ($2.63 \text{ \AA} \times 4$) atoms and eight W(2) atoms ($2.95 \text{ \AA} \times 8$) form a distorted hexagonal antiprism (ASRS). Two W(1) atoms ($2.48 \text{ \AA} \times 2$) complement it by caps over hexagonal faces. In the second coordination sphere (Fig. 16e) four Si(1) atoms ($4.82 \text{ \AA} \times 4$) form a square.

InNi_2 (120). The structural ensemble is a bispheric complex with an Ni(1) atom in the center. The first coordination sphere (Fig. 17a) consists of In atoms ($2.73 \text{ \AA} \times 6$) and Ni(2) atoms ($2.73 \text{ \AA} \times 6$), which are positioned at the vertices of a hexagonal prism so that In and Ni atoms alternate at the vertices of the hexagonal faces and every In atom is in contact with Ni atoms in the neighboring hexagonal prism. In the second coordination sphere (Fig. 17b), eight Ni(1) atoms ($2.57 \text{ \AA} \times 2$, $4.18 \text{ \AA} \times 6$) form a hexagonal bipyramid, which is a polyhedron dual to the preceding one.

CaIn_2 (128). The structural ensemble consists of one complex with two coordination spheres. It is similar to that of InNi_2 . In the center of the complex is a Ca atom. The first coordination sphere (Fig. 18a) is formed by In atoms ($3.23 \text{ \AA} \times 6$, $3.63 \text{ \AA} \times 6$), which are situated at the vertices of a distorted hexagonal prism. All the edges of the hexagonal faces are $2.91 \text{ \AA} \times 12$, *i.e.* a little shorter than the shortest distances in metallic indium (3.25 \AA). The edges of the polyhedron connecting the hexagonal faces have different lengths: $3.18 \text{ \AA} \times 3$ and $4.57 \text{ \AA} \times 3$ and the long edges alternate with the short ones.

In the second coordination sphere (Fig. 18b), eight Ca atoms ($3.82 \text{ \AA} \times 2$, $4.90 \text{ \AA} \times 6$) form a polyhedron dual to the preceding one, *i.e.* a hexagonal bipyramid.

CeCu_2 (110). The structure type CeCu_2 is similar to the structure type InNi_2 , not taking the distortions

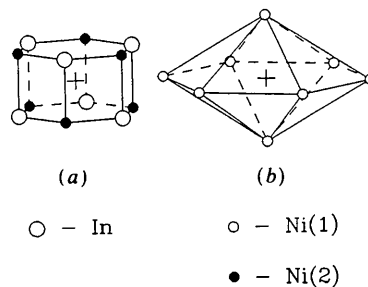


Fig. 17. Structural ensemble InNi_2 . Atom Ni(1) is at the center: (a) and (b) the first and second coordination spheres.

into account. The structural ensemble of CeCu_2 is monocomplex. The complex consists of two coordination spheres and a central Ce atom. In the first coordination sphere (Fig. 19a) the vertices of a slightly distorted hexagonal prism are occupied by Cu atoms ($3.02 \text{ \AA} \times 4$, $3.07 \text{ \AA} \times 2$, $3.11 \text{ \AA} \times 2$ and $3.21 \text{ \AA} \times 4$). The lengths of all edges of the hexagonal faces are essentially equal to the interatomic distance in pure copper (2.55 \AA): $(1-3) = (1-4) = (2-5) = (2-6) = 2.55 \text{ \AA}$; $(3-9) = (4-10) = (5-11) = (6-12) = 2.56 \text{ \AA}$; $(7-9) = (7-10) = (8-11) = (8-12) = 2.55 \text{ \AA}$. But the lengths of the edges connecting the hexagonal faces differ widely: $(1-2) = (3-5) = (4-6) = 4.24 \text{ \AA}$; $(7-8) = (9-11) = (10-12) = 2.81 \text{ \AA}$. The cause of these distortions is difficult to explain.

In the second coordination sphere (Fig. 19b) of the complex, eight Ce atoms (apical atoms: $3.57 \text{ \AA} \times 2$; equatorial atoms: $3.86 \text{ \AA} \times 2$, $4.43 \text{ \AA} \times 2$ and $4.83 \text{ \AA} \times 2$) are placed at the vertices of a distorted hexagonal bipyramid, *i.e.* the polyhedra of the first and second coordination spheres are dual to each other.

(c) Compounds with other compositions

CFe_3 . The structural ensemble consists of one bispheric complex with a C atom in the center. In the first coordination sphere (Fig. 20a), the Fe atoms form a distorted gyroelongated tetragonal pyramid (ZP no. 10) with the following atoms in the vertices of the antiprism: Fe(1) ($2.01 \text{ \AA} \times 2$); Fe(2) ($2.02 \text{ \AA} \times 4$), Fe(2) ($2.38 \text{ \AA} \times 2$) and the Fe(1) (2.81 \AA) in the

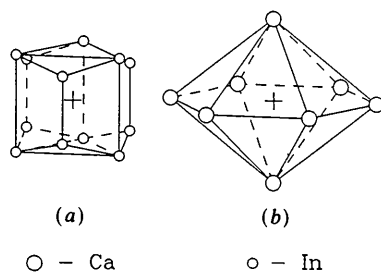


Fig. 18. Structural ensemble CaIn_2 . The Ca atom is at the center: (a) and (b) the first and second coordination spheres.

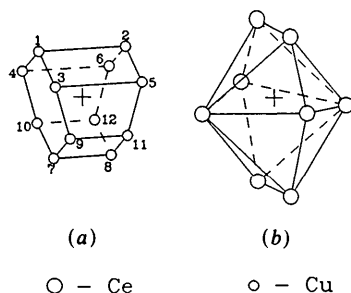


Fig. 19. Structural ensemble CeCu_2 . The Ce atom is at the center: (a) and (b) the first and second coordination spheres.

cap vertex. This polyhedron may also be described as a distorted triaugmented trigonal prism (ZP no. 51). The real polyhedron is intermediate between these two ideal polyhedra. In the second coordination sphere (Fig. 20b), the C atoms ($3.03 \text{ \AA} \times 2$, $3.64 \text{ \AA} \times 2$ and $3.85 \text{ \AA} \times 2$) form a distorted octahedron.

Ni_3Sn (86). The structural ensemble consists of one bispheric complex with an Sn atom at the center. In the first coordination sphere (Fig. 21a), the Ni atoms form an anticuboctahedron ($2.61 \text{ \AA} \times 6$, $2.64 \text{ \AA} \times 6$) and, in the second one (Fig. 21b), the Sn atoms are positioned at the vertices of an elongated trigonal bipyramid ($3.72 \text{ \AA} \times 6$, $4.24 \text{ \AA} \times 2$).

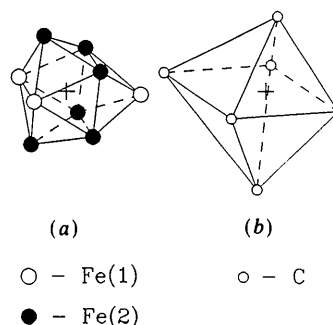


Fig. 20. Structural ensemble CFe_3 . The C atom is at the center: (a) and (b) the first and second coordination spheres.

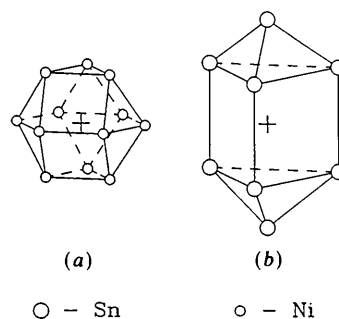


Fig. 21. Structural ensemble Ni_3Sn . The Sn atom is at the center: (a) and (b) the first and second coordination spheres.

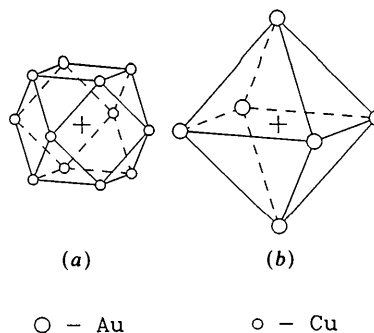


Fig. 22. Structural ensemble AuCu_3 . The Au atom is at the center: (a) and (b) the first and second coordination spheres.

AuCu_3 (386). The structural ensemble consists of one bispheric complex with an Au atom at the center. In the first coordination sphere (Fig. 22a) the Cu atoms ($2.65 \text{ \AA} \times 12$) are distributed at the vertices of a cuboctahedron and in the second one (Fig. 22b) the Au atoms ($3.75 \text{ \AA} \times 6$) occupy the vertices of an octahedron.

AuCu (93). The structural ensemble consists of one bispheric complex centered on the atom Au(1) (the same complex exists around the Cu atom). In the first coordination sphere (Fig. 23a), the Cu atoms ($2.70 \text{ \AA} \times 8$) and Au(2) atoms ($2.80 \text{ \AA} \times 4$) are distributed at the vertices of a slightly distorted cuboctahedron. In the second coordination sphere (Fig. 23b), Au(1) atoms ($3.67 \text{ \AA} \times 2$, $3.97 \text{ \AA} \times 4$) are at the vertices of an octahedron slightly compressed along one of the fourfold axes.

$\text{Mn}_{23}\text{Th}_6$ (108). The structural ensemble consists of one multispheric complex, its center is occupied by an Mn(1) atom. In the first coordination sphere (Fig. 24a), the Mn(3) atoms ($2.65 \text{ \AA} \times 8$) form a cube; in the second (Fig. 24b), the Th atoms ($3.72 \text{ \AA} \times 6$) are situated at the vertices of an octahedron; in the third (Fig. 24c), the Mn(2) atoms ($4.43 \text{ \AA} \times 12$) form a cuboctahedron; in the fourth (Fig. 24d), a distorted rhombicuboctahedron is formed by Mn(4) atoms ($5.12 \text{ \AA} \times 24$); in the fifth (Fig. 24e), the Th atoms ($6.76 \text{ \AA} \times 24$) are at the vertices of a truncated octahedron; in the sixth (Fig. 24f), a truncated cube consists of Mn(3) atoms ($6.87 \text{ \AA} \times 24$); in the seventh (Fig. 24g), there is a cube with Mn(4) atoms ($6.98 \text{ \AA} \times 8$) at the vertices; in the eighth (Fig. 24h), there is a rhombicuboctahedron with Mn(2) atoms ($7.67 \text{ \AA} \times 24$) at the vertices; the ninth (Fig. 24i) contains an octahedron, with vertices occupied by Th atoms ($8.80 \text{ \AA} \times 6$); in the tenth (Fig. 24j) there is a cuboctahedron with Mn(1) atoms ($8.56 \text{ \AA} \times 12$) at the vertices.

AgAsMg (99). The structural ensemble consists of one bispheric complex with an As atom at the center. In the first coordination sphere (Fig. 25a), the Ag

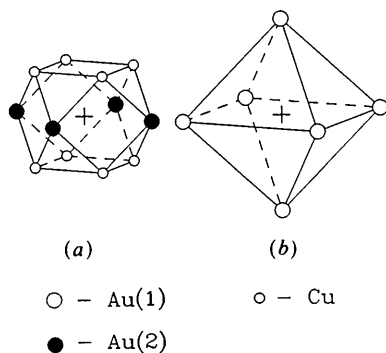


Fig. 23. Structural ensemble AuCu. Atom Au(1) is at the center: (a) and (b) the first and second coordination spheres.

atoms ($2.71 \text{ \AA} \times 4$) and Mg atoms ($2.71 \text{ \AA} \times 4$) form a cube in common, but atoms of each element form tetrahedra. In the second coordination sphere (Fig. 25b), the As atoms ($4.42 \text{ \AA} \times 12$) form a cuboctahedron.

AuBe_5 (52). The structural ensemble consists of one five-spheric complex centered on the Be(1) atom. In the first coordination sphere (Fig. 26a), the Be(2) atoms ($2.08 \text{ \AA} \times 12$) form a cuboctahedron; in the second (Fig. 26b), the Au atoms ($2.64 \text{ \AA} \times 4$) are positioned at the vertices of a tetrahedron; in the third (Fig. 26c), the Be(2) atoms ($3.23 \text{ \AA} \times 12$) form a cuboctahedron; in the fourth (Fig. 24d), the same Be(2) atoms ($3.89 \text{ \AA} \times 48$) are at the vertices of a distorted truncated cuboctahedron; in the fifth (Fig. 26e), the Be(1) atoms ($4.31 \text{ \AA} \times 12$) are distributed at the vertices of a cuboctahedron.

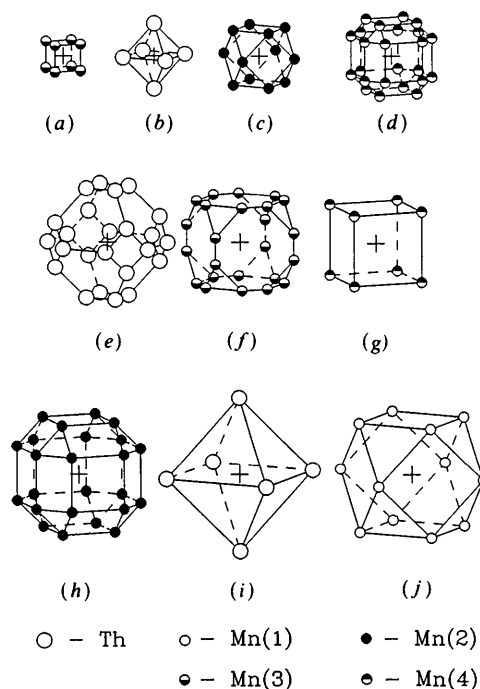


Fig. 24. Structural ensemble $\text{Mn}_{23}\text{Th}_6$. Atom Mn(1) is at the center: (a)-(j) the coordination spheres (the description is in the text).

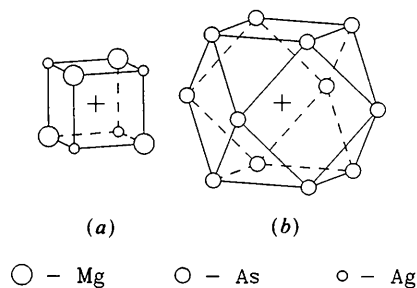


Fig. 25. Structural ensemble AgAsMg. The As atom is at the center: (a) and (b) the first and second coordination spheres.

(d) *Crystal and quasicrystal of NiTi₂ (60)*

The structural ensemble of the crystal NiTi₂ consists of one bispheric complex with an atom Ti(1) at the center. The atoms Ni (2.48 Å × 6) and Ti(2) (2.94 Å × 6) are distributed at the vertices of the distorted icosahedron (Fig. 27a) in the first coordination sphere. There is a dual polyhedron, a dodecahedron (Fig. 27b) as a second coordination sphere with the atoms Ti(1) (4.00 Å × 6), Ni (4.18 Å × 2) and Ti(2) (4.53 Å × 12) at the vertices. There are two tetrahedral fragments of the dodecahedron, formed by the atoms

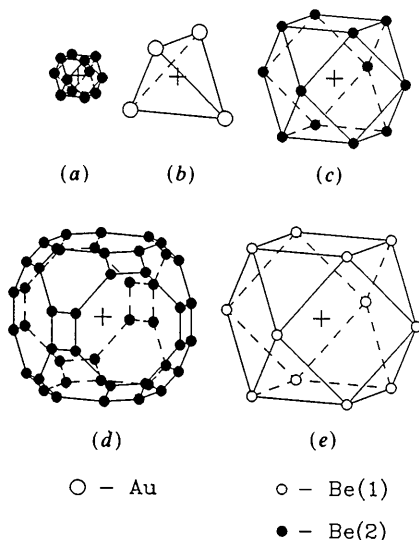


Fig. 26. Structural ensemble AuBe₅. Atom Be(1) is at the center: (a)-(e) the first to fifth coordination spheres.

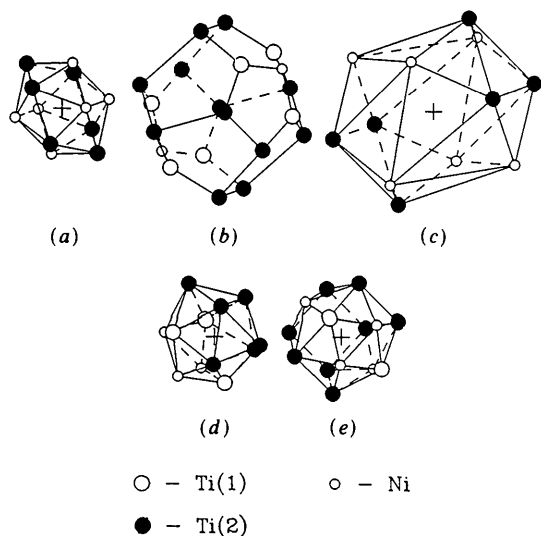


Fig. 27. Structural ensemble NiTi₂. Atom Ti(1) is in the center: (a), (b) and (c) the first to third coordination spheres; (d) the coordination polyhedron of atom Ni; (e) the coordination polyhedron of atom Ti(2).

Ti(1) only if the central atom Ti(1) is. These tetrahedra have a common vertex (the central atom). All tetrahedra made of the atoms Ti(1) are involved in a three-dimensional network running through the crystal.

The third coordination sphere (Fig. 27c) is very important for realization of the problem of the quasicrystal formation NiTi₂. It is a distorted icosahedron which is dual to the dodecahedron of the second coordination sphere and consists of atoms Ni (5.20 Å × 6) and Ti(2) (5.37 Å × 6). The triangular faces of this icosahedron cover all atoms of the second coordination sphere in such a way that each atom of the second sphere is surrounded by nine atoms, positioned at the vertices of the distributed icosahedron fragment, *i.e.* three atoms of the icosahedral face of the first coordination sphere, three atoms of the second coordination sphere connected with the atom under consideration by the dodecahedral edges and three atoms of the icosahedral face in the third coordination sphere. These nine atoms are completed with triple atoms up to an icosahedron for atoms Ti(1) and Ni (Fig. 27a and 27d respectively), but the close environment of atom Ti(2) contains five additional atoms producing a polyhedron with 14 vertices (Fig. 27e), hebesphenomegacoroná (ZP no. 89).

In spite of the resemblance of the first coordination spheres of polyhedra, there is a difference in coordination spheres for atoms Ti(1) and Ni: the latter has only one coordination sphere [as many as Ti(2)] in contrast to Ti(1). So the sequence of the three coordination spheres with the icosahedral symmetry polyhedra around atom Ti(1) is a precondition for a quasicrystal phase.

Concluding remarks

The analysis of the widespread structural types of intermetallic phases shows that the CCMAI corresponds to the crystal structures of these inorganic compounds satisfactorily. This and the previous papers (Aslanov, 1988a, b, 1989a, b, 1991; Aslanov & Markov, 1989) demonstrate that one can describe the crystal structures using PRS, ASRS and ZP. A few exceptions to this rule can be explained on the basis of atomic interaction energies in the way used above for the unusual polyhedra of Ba, Th and Ca atoms in the structures Al₄Ba, ThMn₁₂ and CaCu₅ respectively: the unusual polyhedra are the result of the balance between the maximal coordination number of the central atom and the maximal energy of the central-atom interaction with each atom of the first coordination sphere.

The reason for the distortions of PRS, ASRS and ZP in many structures is the same as that for the formation of unusual polyhedra. The distortion of the monospheric polyhedron-like hexagonal prism

(CaIn₂, CeCu₂) or anticuboctahedron (Ni₃Sn) to multispheric polyhedra gives the maximal total energy of the atomic interaction between the central atom and the first coordination sphere because of the maximal coordination number.

It is worth noting that many ZP are bispheric and presumably this property is essential for the maximal coordination number and for the gain in total energy of the atomic interactions.

The intermetallic structures have many examples of dual polyhedra in adjacent coordination spheres. This is one of the important properties of these structures in contrast to the structures of the ionic compounds.

References

- ASLANOV, L. A. (1988a). *Acta Cryst.* B44, 449-458.
 ASLANOV, L. A. (1988b). *Acta Cryst.* B44, 458-462.
 ASLANOV, L. A. (1989a). *Acta Cryst.* A45, 671-678.
 ASLANOV, L. A. (1989b). *Structures of Substances*. Moscow Univ. Press (in Russian).
 ASLANOV, L. A. (1991). *Acta Cryst.* A47, 63-70.
 ASLANOV, L. A. & MARKOV, V. T. (1989). *Acta Cryst.* A45, 661-671.
 VILLARS, P. & CALVERT, L. D. (1985). *Pearson's Handbook of Crystal Data for Intermetallic Phases*, Vol. I. Metals Park, OH: American Society for Metals.
 WELLS, A. F. (1984). *Structural Inorganic Chemistry*. Oxford: Clarendon Press.
 ZALGALLER, V. A. (1969). *Convex Polyhedra with Regular Faces*. New York: Consultants Bureau.

Acta Cryst. (1992). A48, 293-301

***Ab Initio* Phase Determination for Viruses with High Symmetry: a Feasibility Study**

BY JUN TSAO,* MICHAEL S. CHAPMAN† AND MICHAEL G. ROSSMANN

Department of Biological Sciences, Purdue University, West Lafayette, Indiana 47907, USA

(Received 22 July 1991; accepted 5 November 1991)

Abstract

Conditions that would permit the complete structure determination of spherical viruses that have high internal symmetry were examined starting only from an initial spherical shell model. Problems were considered that might arise due to the following. 1. Creation of centric phases due to the simple shell model and its position in the unit cell. The centric symmetry can generally be broken on averaging an initial electron density map based on observed structure amplitudes, provided that the internal molecular symmetry is sufficiently non-parallel to the crystallographic symmetry. 2. Choice of the average model shell radius. Some incorrect radii led to the Babinet opposite solution (electron density is negative instead of positive). Phases derived from other models with incorrect radii failed to converge to the correct solution. 3. Error in structure amplitude measurements. 4. Lack of a complete data set. 5. Error in positioning the initial spherical-shell model within the crystal unit cell. It was found that an error of 1.6 Å caused noticeable phasing error at a resolution greater than 20 Å.

Introduction

There is now abundant literature on the refinement and extension of phases to higher resolution in the presence of noncrystallographic symmetry (Rossmann, 1990; Bricogne, 1974). Use of the power of noncrystallographic symmetry is particularly applicable in the structure determination of icosahedral viruses because they possess ample symmetry, including fivefold axes which can only be local in nature. However, noncrystallographic symmetry is also used more and more frequently in the structure determination of oligomeric proteins or proteins that can be induced to crystallize in more than one crystal form. Here we explore the feasibility of extending phases derived from a very simple low-resolution model to high resolution. The effects of various errors on such phasing were examined theoretically by Arnold & Rossmann (1986). We examine experimentally the effects of various errors and data defects which may inhibit or retard such phasing. A similar investigation has previously been published by Rayment (1983). However, we emphasize, the requirements for phase extension to higher (3 Å) resolution as well as errors in molecular positioning that have not previously been considered.

Spherical-virus-structure determinations have depended on the use of noncrystallographic symmetry

* Current address: Department of Biochemistry, Center for Macromolecular Crystallography, 262BHS, THT 79, University of Alabama, University Station, Birmingham, Alabama 35294, USA.

† To whom correspondence should be addressed.